Transmission electron microscopy (TEM) characterisation of Ru_2Si_3 thin films formed by solid state reaction of Ru and Si

G.K.H. Pang[a], M.G. Blackford[b] and Emil.V. Jelenković[c]

[a] *Process Engineering and Light Metals Centre, Central Queensland University, Bryan Jordan Drive, Gladstone, Queensland 4680, Australia.*
[b] *Institute of Materials and Engineering Science, Australian Nuclear Science and Technology Organisation, PMB 1, Menai, NSW 2234, Australia.*
[c] *Department of Electronic and Information Engineering, The Hong Kong Polytechnic University, Hong Kong, People's Republic of China.*

Transmission electron microscopy investigation on Ru_2Si_3 thin films formed by solid state reaction of Ru and Si revealed a top layer of SiO_2 with embedded Ru clusters. We attribute the formation of the top layer to the oxidation between residual oxygen traces in the nitrogen and the silicon in Ru_2Si_3 grains. The observation is in agreement with electrical measurements. In addition, an interlayer, which has complex structure and chemistry, was observed between the film and substrate.

1. Introduction

In the recent years, Ru_2Si_3 growth on silicon has been fabricated for the applications as LED in the infra red region [1-5]. Among the different methods, sputtering has been proved as a successful technique to fabricate the heterostructure Ru_2Si_3 diodes by solid state reaction between deposited Ru and Si through post-annealing [5]. XRD spectrum indicates that all Ru transforms into Ru_2Si_3; however, the structure of the films has not been fully understood. For instance, it was reported that the resistivity of Ru_2Si_3 film reduces from about 10 Ω cm to 0.1 Ω cm after a dip in HF solution [3,5]. Lessen *et* al [3] attribute the phenomenon to hydrogen passivation of the dangling bonds. The HF solution passivates the dangling bonds and removes the potential barriers. On the other hand, Jelenkovic *et al* [5] speculate that oxygen trace in the annealing process causes the oxidation of Ru_2Si_3. The HF solution thus removes the surface oxide and leads to the reduction in resistivity. The other structural issue of the Ru_2Si_3 film arises from the complexity of the Ru-Si phase diagram; the interface between the evaporated Ru film and the silicon substrate has shown to be complicated [6]. It is therefore expected that the interface between the silicon substrate and Ru_2Si_3 films formed by the sputtering and post-annealing method will also lead to the formation of complicated interface. The aim of the TEM study is to investigate the structure of the Ru_2Si_3 films in particular at the surface and the interface between the substrate.

2. Experimental

A cross-sectional TEM sample was prepared by the usual method that involved grinding and polishing until its thickness was less than 10 microns. Ion milling was performed using Gatan PIPS Ion miller. Transmission electron microscopy (TEM) was performed using a JEOL JEM 2010F (JEOL, Japan) equipped with a field emission gun (FEG) operated at 200kV. The TEM was equipped with an energy dispersive x-ray (EDX) spectrometer and NORAN System SIX microanalysis system (Thermo Electron Corporation, USA) and GIF 2001 electron energy filter (Gatan, USA). All oxygen maps were collected using the O-K edge at 532eV energy loss together with the default setting in the DigitalMicrograph software. The energy selecting slit was 30eV wide and the three images used to create the maps were centred at: post-edge = 547eV, pre-edge 1 = 484eV and pre-edge 2 = 514eV.

3. Results

The bright-field TEM image in Fig. 1(a) shows that the film is about 80 nm thick and is composed of columnar grains 20 – 30 nm across. A layer of 5 – 7 nm thick was found on top of the film and an interlayer of 5 – 7 nm was found between the film and the silicon substrate. EELS elemental mapping was performed in order to study the distribution of elements in the film. Figure 1 (b) shows the EELS oxygen map acquired from the region shown in Fig. 1 (a). The spectrometer was configured to transmit only those electrons which had lost 532 eV due to the excitation of oxygen K-shell electrons in the specimen. The resulting image therefore represents the distribution of oxygen in the region imaged, with brighter areas indicating more oxygen. The resulting oxygen map is rather noisy due to low signal intensity and background correction procedures; however, it shows clearly that the top layer contains oxygen. The bright region in Figure 1(a) above the interlayer at the substrate interface also contains oxygen. Elemental jump ratio mapping provides an alternative technique for visualising the oxygen distribution. An image of 532 eV energy loss is divided by an image of slightly lower energy loss (below the oxygen ionisation energy). The resulting image, Figure 1 (c), clearly shows that the top layer consists of an oxygen rich layer and embedded nano-size clusters, which do not contain oxygen. One of the embedded clusters is marked both in the oxygen-jump image, Fig. 1 (c), and the bright-field image, Fig. 1(a).

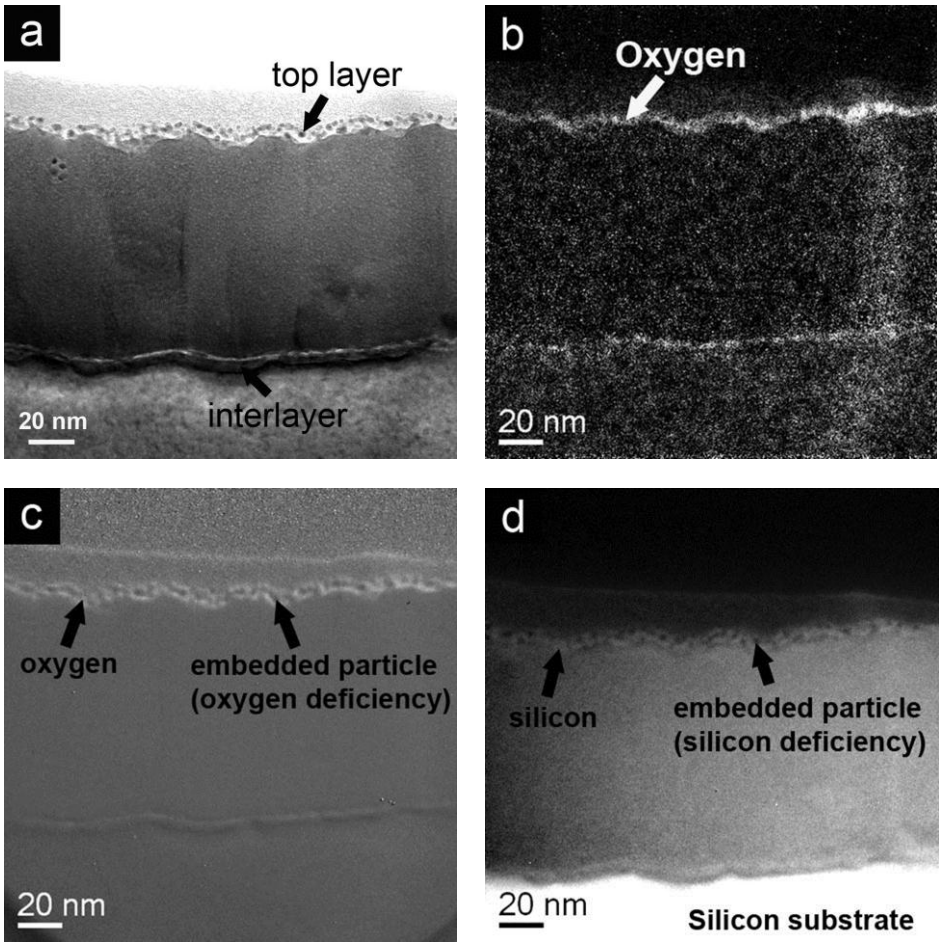

Fig. 1. (a) Bright-field TEM image of Ru_2Si_3/Si showing a top layer and an interlayer as marked. (b) EELS oxygen map showing the presence of the oxygen in the top layer and the interlayer. (c) Elemental jump ratio mapping showing that the top layer consists of an oxygen rich layer and embedded nano-size clusters, which do not contain oxygen. (d) EELS silicon map showing the embedded nano-size clusters do not contain silicon but their surrounding layer is silicon rich.

The distribution of silicon is shown in the EELS map in Figure 1(d). Silicon is detected in the film which is consistent with a fully reacted Ru_2Si_3 film indicated by XRD results. More importantly, the top layer, which contains oxygen, also contains silicon. The clusters embedded in the layer, however, do not show any detectable silicon as indicated by the arrow. The oxygen-jump ratio map and silicon map therefore suggest that the top layer is SiO_2 with embedded Ru clusters in the layer. The interlayer between the film and substrate does not appear to be a single composition. It contains both silicon and oxygen as evidenced by Figures 1(d) and (b), respectively, but there also appears to be a deficiency of Si at the interface between the substrate and interlayer. This may be a residual Ru layer.

Figure 2 shows the high resolution image of the top layer and the upper part of the film. Lattice fringes in the loosely attached nano grains are consistent with the spacing of Ru planes. The HRTEM images support the results from the EELS element mapping; the top layer of the film is composed of 2 – 4 nm nano clusters of Ru embedded in a 7 nm thick SiO_2.

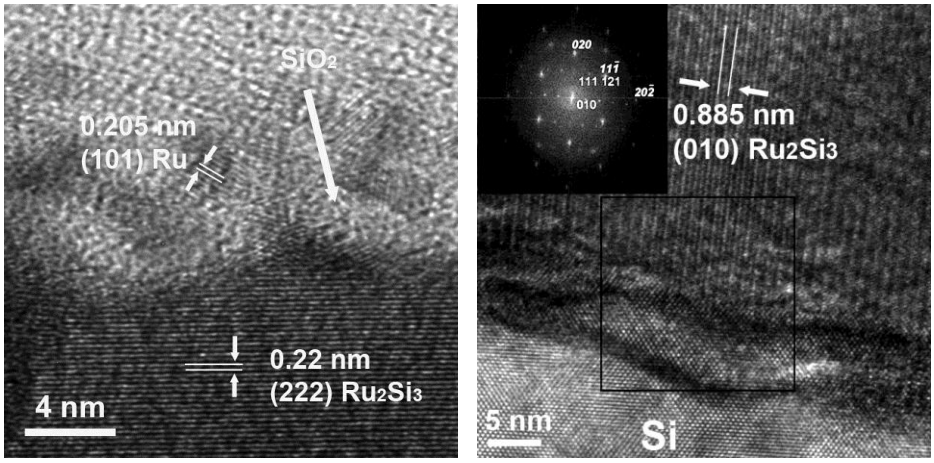

Fig. 2. (Left) HRTEM image of the top layer showing lattice fringes from (101) planes of a Ru embedded in SiO_2. Lattice fringes from (222) planes of a Ru_2Si_3 grain can also be seen.
Fig. 3. (Right) HRTEM image of interface between Ru_2Si_3 and Si showing lattice fringes from (101) planes of Ru_2Si_3.

The interface between the Si substrate and the Ru_2Si_3 film was studied by HRTEM. In Fig. 3 the interface region is marked by a square. The power spectrum of Fast Fourier Transformation is shown in the inset. The two sets of spots associated with lattice planes from Si and Ru_2Si_3 are clearly discernable. The planes corresponding to silicon substrate are labelled with bold italic font. Using the published lattice constants for Ru_2Si_3: a = 1.1057 nm, b = 0.8934 nm, c = 0.5533 nm [7], the (010), (111) and (121) planes are identified and labelled. Using silicon as the calibration, the interplanar distances of the following planes were measured on the HRTEM image as: d_{010} = 0.885 nm and d_{111} = 0.418 nm. They are 1% and 3% less than the values obtained from the lattice constants of Ru_2Si_3, which give d_{010} = 0.8934 nm and d_{111} = 0.4329 nm. The (010) plane of Ru_2Si_3 is 4.7° tilted from plane of Si and it means that (101) plane of Ru_2Si_3 is also 4.7° tilted from (010) plane of silicon, which is the plane for the growth of Ru and Ru_2Si_3 grains. The FFT power spectrum also shows that (121) plane of Ru_2Si_3 is coincident with of Si. The orientation relationship between the Ru_2Si_3 grain and the Si substrate can be described as follows: Ru_2Si_3(101)//Si(001) and Ru_2Si_3[010]//Si with 4.7° mismatched. In addition to the above orientation shown in the figure, other orientation relationships were also observed. It should be note that the lattice fringes from {110} planes of silicon run into the interlayer between the substrate and the film; however, EDS (not show here) indicates that the interlayer contains significant percentage of ruthenium.

4. Conclusion

In summary, the sputtered ruthenium film reacts with silicon completely and forms Ru_2Si_3 film after annealing at 700C in nitrogen for 5 minutes. The Ru_2Si_3 film is about 80 nm thick and is composed of 20 – 30 nm width columns of Ru_2Si_3 grains. A top layer of SiO_2 with embedded Ru clusters, which is about 7 nm thick, was observed. We attribute the formation of the top layer to the oxidation between residual oxygen traces in the nitrogen and the silicon in Ru_2Si_3 grains. The observation support the suggestion given by by Jelenkovic *et al*. [5] on the reduction of resistivity after the samples were dipped in HF suggested. The interlayer between the film and substrate contains silicon and ruthenium as evident from EELS element map and EDS. The interlayer is a complex Ru_xSi_y phase.

Acknowledgments

The authors would like to thank the Australian Institute of Nuclear Science and Engineering for providing financial assistance (Award No 5772) to enable work on TEM experiments to be conducted. The first author thanks Robert Aughterson for his help in preparing the TEM samples. The first author also thanks for the supports of PELM centre of CQU.

References

[1] Chen C C, Yu B H and Liu J F 2009 *Journal of Ceramic Processing Research* **10** 692

[2] Lenssen D, Bay H L, Mesters S, Dieker C, Guggi D, Carius R and Mantl S 1998 *J. Lumin.* **80** 461 doi:10.1016/s0022-2313(98)00148-3

[3] Lenssen D, Carius R, Mantl S and Birdwell A G 2001 *J. Appl. Phys.* **90** 3347

[4] Lenssen D, Carius R, Mesters S, Guggi D, Bay H L and Mantl S 2000 *Microelectron. Eng.* **50** 243

[5] Jelenkovic E V, Tong K Y, Cheung W Y and Wong S P 2003 *Semicond. Sci. Technol.* **18** 454

[6] Pasquali L, Mahne N, Montecchi M, Mattarello V and Nannarone S 2009 *J. Appl. Phys.* **105** doi:10.1063/1.3079507

[7] Poutcharovsky D Jand Parthé E 1974 *Acta Cyrstallography B* **30** 2692